JOURNAL OF THEORETICAL
AND APPLIED MECHANICS
1, **40**, 2002

DYNAMIC ANALYSIS OF LARGE DEFORMATION CONTACT OF ELASTIC BODIES

Gwidon Szefer
Dorota Jasińska

Institute of Structural Mechanics, Cracow Unuversity of Technology
email: szefer@limba.wil.pk.edu.pl

The paper presents numerical calculations of dynamic contact problems in the presence of friction and large deformations. Since this kind of boundary-value problems exhibit a strong nonlinearity, the increments of all contact-dependent terms are discussed in details. Different friction models are considered.

Key words: unilateral contact, friction, large deformations

1. Introduction

In the paper a dynamic unilateral contact problem of elastic bodies subject to large displacements and large deformations in terms of friction will be considered. The formulation and setting of proper contact conditions in this kind of boundary-value problems was discussed by many authors (see He et al., 1996; Klarbing, 1995; Klarbing and Björkman, 1992; Laursen and Simo, 1993a,b; Laursen, 1994; Szefer, 1997, 1998; Szefer et al., 1994; Curnier et al., 1994). Friction (also in the presence of large deformations) was discussed in a common work edited by Raous (1988). The large deformation contact involved with an impact was presented by Wriggers et al. (1990), and Zhong (1993). Difficulties connected with the determination of the unknown contact zone and the lack of the existence theorem for larger friction coefficients (see Jarusek, 1999) constitute, that the dynamic frictional contact of bodies in the presence of finite strains belongs furthermore to the recent problems of the contact mechanics. In the present paper we focus our attention on the numerical analysis demonstrating results for different models of friction (among them also for $\mu > 1$). The paper is organized as follows: we start with a general formulation of the problem in a possibly convenient form, which is stated in Section 2. Next, we pass to the numerical statement connected as well with the strong nonlinearity as with the space and time discretization of the problem. Examples of numerical calculations for kinematic and dynamic excitations are given in Section 4. Concluding remarks summarize the results of the paper.

2. Formulation of the problem

Consider an elastic body B^+ which, due to external body forces with the density $\boldsymbol{b}$ and the prescribed surface tractions $\boldsymbol{p}$, is in contact with another target body B^- (which may be elastic or rigid).

Denote by B_R and B_t the reference and current configurations of the bodies, respectively (Fig. 1). Let $\{0X^K\}$ and $\{0x^i\}$, $i, K = 1, 2, 3$ stand for the material and spatial coordinates of the particles $\boldsymbol{X} \in B_R$. Denote furthermore by ∂B_R^u, ∂B_R^σ these portions of the boundary of B_R, where displacements and tractions are prescribed, and by Γ_c the unknown in advance (except the particular cases) contact zone (Γ_c must be found through the deformation process). Thus, the most convenient statement of the dynamic initial-boundary-value problem in terms of the large deformation takes the form

$$\begin{gathered}
\int\limits_{V_R} T_{iK}\delta u_{i,K}\, dV_R = \int\limits_{V_R} \rho_R b_i \delta u_i\, dV_R + \int\limits_{S_R} p_{iR}\delta u_i\, dS_R - \int\limits_{V_R} \rho_R \ddot{u}_i \delta u_i\, dV_R + \\
+ \int\limits_{\Gamma_c} t_{ci}\delta u_i\, d\Gamma \qquad \forall \delta\boldsymbol{u} \in \mathcal{U}^0 \\
u_i(X^K, t_0) = u_{0i}(X^K) \qquad \dot{u}_i(X^K, t_0) = v_{0i}(X^K)
\end{gathered} \tag{2.1}$$

where

$$V_R = B_R^+ \cup B_R^- \qquad S_R = (\partial B_R^+ \cup \partial B_R^-) \setminus \Gamma_c$$

$$S_R^u = \partial B_R^{+u} \cup \partial B_R^{-u} \qquad \mathcal{U}^0 = \{\delta\boldsymbol{u} : \ \delta\boldsymbol{u} = \boldsymbol{0} \ \text{ on } S_R^u\}$$

and

- T_{Ki} – components of the I Piola-Kirchhoff stress tensor $\mathbf{T}_R$ which satisfy the angular momentum conditions $T_{Ki}(\delta_{jK} + u_{j,K}) = T_{Kj}(\delta_{iK} + u_{i,K})$
- t_{ci} – components of the contact stress vector $\boldsymbol{t}_c$
- $u_i, \delta u_i$ – components of the real and virtual displacement vectors $\boldsymbol{u}$, $\delta\boldsymbol{u}$

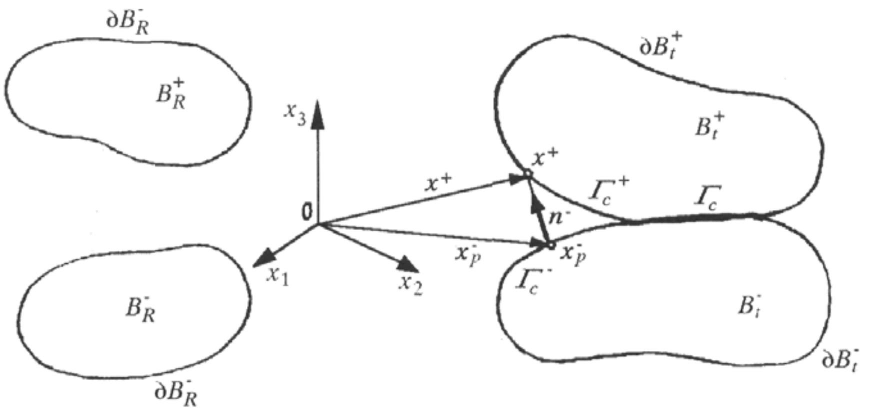

Fig. 1.

More details about the derivation of the virtual power principle in terms of large deformations and a large displacement contact one can find in the papers of Laursen (1994), Laursen and Simo (1993a,b), Szefer et al. (1994). Determination of the contact domain Γ_c and the contact stresses t_c needs setting of the contact conditions. For this reason, a distance (or gap) function must be introduced. Denote by $\Gamma_c^+ \in \partial B_t^+$ and $\Gamma_c^- \in \partial B_t^-$ these parts of the boundaries, which potentially may come into contact at the instant t (see Fig. 1). Assuming large displacements, let us define

$$g_n(\boldsymbol{x}^+, \boldsymbol{x}_p^-) = (\boldsymbol{x}^+ - \boldsymbol{x}_p^-)\boldsymbol{n}^-(\boldsymbol{x}_p^-) \tag{2.2}$$

where

$\boldsymbol{x}_p^-$ – orthogonal projection of $\boldsymbol{x}^+ \in \Gamma_c^+$ onto Γ_c^-, $\boldsymbol{x}_p^- = \mathrm{proj}\boldsymbol{x}^+$

$\boldsymbol{n}^-$ – outward unit vector normal to Γ_c^- at $\boldsymbol{x}_p^-$

The projection vector $\boldsymbol{x}_p$ results from the solution of the system of equations

$$\Big[\boldsymbol{x}^+ - \boldsymbol{x}_p^-(X^K(\theta^\alpha), t)\Big] \cdot \boldsymbol{a}_\alpha = 0 \tag{2.3}$$

where

$$\boldsymbol{a}_\alpha = \frac{\partial \boldsymbol{x}^-}{\partial \boldsymbol{X}^-}\frac{\partial \boldsymbol{X}^-}{\partial \alpha} = (\mathbf{1} + \nabla \boldsymbol{u})\frac{\partial \boldsymbol{X}^-}{\partial \alpha}$$

are basic vectors tangent to the surface Γ_c^- described by the parametric equations $x^i = x^i(X^K(\theta^\alpha), t)$, $\alpha = 1, 2$.

Equations (2.3) can be solved iteratively, only.

To formulate the Signorini unilateral contact conditions the normal component of the Cauchy stress vector $\boldsymbol{t}_c$ must be calculated

$$t_n = \boldsymbol{t}_c \cdot \boldsymbol{n}^- = (\mathbf{T}\boldsymbol{n}^-) \cdot \boldsymbol{n}^- = t_{ji} n_j^- n_i^- = J^{-1} T_{Ki}(\delta_{jK} + u_{j,K}) n_j^- n_j^- \tag{2.4}$$

Here $J = \det(\delta_{ik} + u_{i,k}) > 0$, and T is the Cauchy stress tensor.

Then we have

$$g_n \geqslant 0 \qquad t_n \geqslant 0 \qquad t_n g_n \geqslant 0$$

i.e.

$$\begin{aligned} &g_n > 0 \Rightarrow t_n = 0 \\ &g_n = 0 \Rightarrow t_n > 0 \end{aligned} \tag{2.5}$$

The friction conditions require calculation of the tangent component of $\boldsymbol{t}_c$, which is equal

$$\begin{aligned} \boldsymbol{t}_\tau &= \boldsymbol{t}_c - \boldsymbol{t}_n = \boldsymbol{t}_c - t_n\boldsymbol{n}^- = \boldsymbol{t}_c - (\boldsymbol{t}_c \cdot \boldsymbol{n}^-)\boldsymbol{n}^- = \\ &= (\mathbf{1} - \boldsymbol{n}^- \otimes \boldsymbol{n}^-)\boldsymbol{t}_c = \mathsf{P}J^{-1}\mathsf{T}_R(\mathbf{1} + \nabla\boldsymbol{u})\boldsymbol{n}^- \end{aligned} \tag{2.6}$$

The second-order tensor $\mathsf{P} = \mathbf{1} - \boldsymbol{n}^- \otimes \boldsymbol{n}^-$ maps any vector $\boldsymbol{t}_c$ to its projection on the plane tangent to the surface Γ_c at the point $\boldsymbol{x}_p^-$.

Hence, the Coulomb-Amonton friction law reads

$$\begin{aligned} &|\boldsymbol{t}_\tau| < \mu t_n \Rightarrow \boldsymbol{v}_T = \mathbf{0} \\ &|\boldsymbol{t}_\tau| = \mu t_n = t_T \Rightarrow \boldsymbol{v}_T = -|\boldsymbol{v}_T|\boldsymbol{e}_T \\ &\boldsymbol{e}_T = \frac{\boldsymbol{t}_T}{\mu t_n} \end{aligned} \tag{2.7}$$

on Γ_c, where $\boldsymbol{v}_T$ is the sliding velocity

$$\begin{aligned} \boldsymbol{v}_T &= [(\dot{\boldsymbol{x}}^+ - \dot{\boldsymbol{x}}_p^-)\boldsymbol{a}_\alpha] = (\boldsymbol{v}^+ - \boldsymbol{v}^-) - [(\boldsymbol{v}^+ - \boldsymbol{v}^-)\cdot\boldsymbol{n}^-]\boldsymbol{n}^- = \\ &= (\mathbf{1} - \boldsymbol{n}^- \otimes \boldsymbol{n}^-)(\boldsymbol{v}^+ - \boldsymbol{v}^-) = \mathsf{P}(\boldsymbol{v}^+ - \dot{\boldsymbol{v}}^-) \end{aligned}$$

and $\mu = \mu(t_n, |\boldsymbol{v}_T|)$ – friction coefficient.

The multivalued relations $t_n = t_n(g_n)$ and $t_{T\alpha} = t_{T\alpha}(v_{T\alpha})$ described by (2.5) and (2.7) are obviously replaced by their regularizations

$$\begin{aligned} &t_{n\varepsilon} = \begin{cases} 0 & g_n > 0 \\ -\dfrac{g_n}{\varepsilon} & g_n \leqslant 0 \end{cases} \qquad \boldsymbol{t}_{T\varepsilon} = -\mu t_n \boldsymbol{\phi}_\varepsilon \\ &\boldsymbol{\phi}_\varepsilon = \begin{cases} \dfrac{\boldsymbol{v}_T}{|\boldsymbol{v}_T|} & |\boldsymbol{v}_T| > \varepsilon \\ \dfrac{\boldsymbol{v}_T}{\varepsilon} & |\boldsymbol{v}_T| \leqslant \varepsilon \end{cases} \end{aligned} \tag{2.8}$$

Instead of (2.5) and (2.7), the compliance model is sometimes used (see Oden and Martins, 1985). Then it is

$$t_n = c_N g_+^{m_N} \qquad g_+ = \begin{cases} 0 & g_n > 0 \\ g_n & g_n \geqslant 0 \end{cases}$$
$$\boldsymbol{t}_T = -c_T g_+^{m_T} \frac{\boldsymbol{v}_T}{|\boldsymbol{v}_T|} \tag{2.9}$$

Taking (2.4)-(2.8) or (2.9) into account we obtain the virtual power of the contact response (the last term in (2.1))

$$\delta L_c = \int\limits_{\Gamma_c} t_{ci}\delta u_i \, d\Gamma = \int\limits_{\Gamma_c} t_n \delta u_n \, d\Gamma + \int\limits_{\Gamma_c} t_{T\alpha}\delta u_{T\alpha} \, d\Gamma \tag{2.10}$$

where

$\delta u_n = (\delta\boldsymbol{u}^+ - \delta\boldsymbol{u}^-)\boldsymbol{n}^-$

$\delta u_{T\alpha} = (\delta\boldsymbol{u}^+ - \delta\boldsymbol{u}^-)\boldsymbol{a}_\alpha$ in the local coordinate system $(\alpha = 1,2)$ or

$\delta u_{Ti} = (\delta\boldsymbol{u}^+ - \delta\boldsymbol{u}^-)\boldsymbol{e}_i$ in the global system $\{0x^i\} i = 1,2,3$.

Since the constitutive equation for the nonlinear elastic material is rather given by the II Piola-Kirchhoff stress tensor $\mathbf{S}$ in the form

$$\mathbf{S} = \frac{\partial W}{\partial \mathbf{E}} = \mathcal{F}(\mathbf{E}) \tag{2.11}$$

where $W = W(\mathbf{E})$ is the elastic potential and

$$\mathbf{E} = (E_{KL}) = \frac{1}{2}(u_{K,L} + u_{L,K} + u_{N,K}u_{N,L}) \tag{2.12}$$

is the Green strain tensor, the relation between $\mathbf{S}$ and $\mathbf{T}_R$ must be introduced

$$T_{Ki} = S_{KL}(\delta_{iL} + u_{i,L}) \tag{2.13}$$

The nonlinearity of (2.1) causes that the incremental approach is obviously used. Thus, considering the sequence of configurations $B_0 = B_R, B_1, ..., B_N, B_{N+1}, ..., B_t$ and introducing the expressions

$$
\begin{aligned}
&\boldsymbol{u}^{N+1} = \boldsymbol{u}^N + \Delta\boldsymbol{u} && \mathbf{T}_R^{N+1} = \mathbf{T}_R^N + \Delta\mathbf{T}_R\\
&\Delta\mathbf{T}_R = \Delta\mathbf{S}(\mathbf{1} + \nabla\boldsymbol{u}) + \mathbf{S}\nabla(\Delta\boldsymbol{u}) && \Delta\mathbf{S} = \mathbf{C}^t\Delta\mathbf{E}\\
&\Delta\mathbf{E} = \frac{1}{2}\Big[\nabla(\Delta\boldsymbol{u}) + \nabla^\top(\Delta\boldsymbol{u}) + \nabla(\Delta\boldsymbol{u})\boldsymbol{u} + \boldsymbol{u}^\top\nabla(\Delta\boldsymbol{u})\Big]\\
&t_n^{N+1} = t_n^+ + \Delta t_n && \boldsymbol{t}_T^{N+1} = \boldsymbol{t}_T^N + \Delta\boldsymbol{t}_T\\
&\Delta t_n = \Delta t_{n\varepsilon} = -\frac{1}{\varepsilon}\Delta g_n = -\frac{1}{\varepsilon}\Delta u_n && g_n \leqslant 0\\
&\Delta\boldsymbol{t}_T = \Delta\boldsymbol{t}_{T\varepsilon} = -(\Delta\mu t_n + \mu\Delta t_n)\boldsymbol{\phi}_\varepsilon - \mu t_n\Delta\boldsymbol{\phi}_\varepsilon\\
&\Delta\boldsymbol{\phi}_\varepsilon = \begin{cases} 0 & |\boldsymbol{v}_T| > \varepsilon\\[2mm] \dfrac{\Delta\boldsymbol{v}_T}{\varepsilon} & |\boldsymbol{v}_T| \leqslant \varepsilon\end{cases}\\
&\boldsymbol{b}^{N+1} = \boldsymbol{b}^N + \Delta\boldsymbol{b} && \boldsymbol{p}_R^{N+1} = \boldsymbol{p}_R^N + \Delta\boldsymbol{p}
\end{aligned}
\tag{2.14}
$$

($\mathbf{C}^t$ – means tangent Hooke's coefficient tensor) we obtain from (2.1) (taking (2.10) into account) the linearised (with respect to the increment $\Delta\boldsymbol{u}$) equation

$$
\begin{aligned}
\int\limits_{V_R} \Delta\mathbf{T}_R : \delta\nabla(\Delta\boldsymbol{u})\,dV_R &= \int\limits_{V_R} \rho_R\Delta\boldsymbol{b}_R\cdot\delta\Delta\boldsymbol{u}\,dV_R + \int\limits_{S_R} \Delta\boldsymbol{p}_R\cdot\delta\Delta\boldsymbol{u}\,dS_R -\\
&- \int\limits_{V_R} \rho_R\Delta\ddot{\boldsymbol{u}}\cdot\delta\Delta\boldsymbol{u}\,dV_R + \int\limits_{\Gamma_c} \Delta t_n\delta\Delta u_n\,d\Gamma + \int\limits_{\Gamma_c} \Delta\boldsymbol{t}_T\cdot\delta\Delta\boldsymbol{u}_T\,d\Gamma + \delta L_{\Delta\Gamma_c}
\end{aligned}
\tag{2.15}
$$

where the term

$$
\begin{aligned}
\delta L_{\Delta\Gamma_c} &= \int\limits_{\Gamma_c}\Big(\frac{\partial t_n}{\partial n} - 2kt_n\Big)\Delta\boldsymbol{\varphi}\cdot\boldsymbol{n}\delta\Delta u_n\,d\Gamma + \int\limits_{\partial\Gamma_c} t_n\boldsymbol{\nu}\cdot\Delta\boldsymbol{\varphi}\delta\Delta u_n\,ds +\\
&+ \int\limits_{\Gamma_c}\Big(\frac{\partial\boldsymbol{t}_T}{\partial n} - 2k\boldsymbol{t}_T\Big)\Delta\boldsymbol{\varphi}\cdot\boldsymbol{n}\delta\Delta\boldsymbol{u}_T\,d\Gamma + \int\limits_{\partial\Gamma_c} \boldsymbol{t}_T\boldsymbol{\nu}\cdot\Delta\boldsymbol{\varphi}\delta\Delta\boldsymbol{u}_T\,ds
\end{aligned}
\tag{2.16}
$$

is the increment of the virtual power which results from the increment (variation) of the contact zone Γ_c (see Szefer, 1997, 1998).

Here $\Delta\boldsymbol{\phi}$ is the increment of the contact domain Γ_c, k – mean curvature of the surface Γ_c, ν – outward unit vector tangent to the surface Γ_c and normal to its boundary $\partial\Gamma_c$.

Equation (2.15) constitutes the basis for numerical analysis of the contact problem.

3. Discretization. Numerical solution of the problem

To solve initial-boundary-value problem (2.1) with contact and friction conditions (2.8), incremental formulation (2.15) has been applied. To solve the problem in increments the space discretization by means of the finite-element technique will be used. Thus, we approximate the solution $u_i(\boldsymbol{X},t)$ (and Δu_i respectively) $i=1,2,3$ in terms of the shape functions $N_{i\alpha}(\boldsymbol{X})$ and nodal displacements $q_\alpha(t)$, $\alpha=1,...,N_e$ as

$$\begin{aligned} u_i(\boldsymbol{X},t) &= \sum_{\alpha=1}^{N} N_{i\alpha}(\boldsymbol{X})q_\alpha(t) = [N_{i\alpha}][q_\alpha] \\ \Delta u_i &= [N_{i\alpha}][q_\alpha] \qquad\qquad \Delta\boldsymbol{u} = \mathbf{N}\Delta\boldsymbol{q} \end{aligned} \tag{3.1}$$

Hence, it will be (respecting the tensor notation)

$$\begin{aligned}
& v_i = \dot{u}_i = [N_{i\alpha}][\dot{q}_\alpha] \qquad\qquad \mathbf{P} = [P_{ij}] = [(\mathbf{1} - \boldsymbol{n}^- \otimes \boldsymbol{n}^-)_{ij}] \\
& \boldsymbol{v}_T = \mathbf{P}(\boldsymbol{v}^+ - \boldsymbol{v}_p^-) \qquad\qquad v_{Ti} = [P_{ij}][N_{j\alpha}][\dot{q}_\alpha^+ - \dot{q}_\alpha^-] \\
& \Delta v_{Ti} = [P_{ij}][N_{j\alpha}][\Delta\dot{q}_\alpha^+ - \Delta\dot{q}_\alpha^-] \\
& \Delta\ddot{u}_i = [N_{i\alpha}][\Delta\ddot{q}_\alpha] \qquad\qquad \Delta u_n = \Delta\boldsymbol{u}\cdot\boldsymbol{n}^- = N_{i\alpha}\Delta q_\alpha n_i \\
& \Delta t_{n\varepsilon} = -\frac{1}{\varepsilon}\Delta u_n = -\frac{1}{\varepsilon}N_{i\alpha}n_i\Delta q_\alpha \\
& t_n = -\frac{u_n}{\varepsilon} = -\frac{1}{\varepsilon}N_{i\alpha}n_i q_\alpha \\
& \Delta\boldsymbol{t}_T = -(\Delta\mu t_n + \mu\Delta t_n)\boldsymbol{\phi}_\varepsilon - \mu t_n\Delta\boldsymbol{\phi}_\varepsilon = \\
& \qquad = -\Delta\mu t_n\boldsymbol{\phi}_\varepsilon + \frac{\mu}{\varepsilon}\boldsymbol{\phi}_\varepsilon N_{j\alpha}n_j\Delta q_\alpha - \frac{\mu t_n}{\varepsilon}\Delta\boldsymbol{v}_T \\
& \boldsymbol{\phi}_\varepsilon = \phi_\varepsilon\boldsymbol{v}_T = \phi_\varepsilon[P_{ij}][N_{j\alpha}][\dot{q}_\alpha^+ - \dot{q}_\alpha^-] \\
& \phi_\varepsilon = \begin{cases} \dfrac{1}{|\boldsymbol{v}_T|} & |\boldsymbol{v}_T| > \varepsilon \\ \dfrac{1}{\varepsilon} & |\boldsymbol{v}_T| \leqslant \varepsilon \end{cases} \\
& t_{Ti} = -\mu t_n\phi_\varepsilon v_{Ti} = -\frac{\mu\phi_\varepsilon}{\varepsilon}N_{j\alpha}n_j q_\alpha[P_{ik}][N_{k\beta}][\dot{q}_\beta^+ - \dot{q}_\beta^-]
\end{aligned} \tag{3.2}$$

The corresponding increments of the considered tensors take the form

$$
\begin{aligned}
\Delta\mathbf{E} &= [\Delta E_{MN}] = \frac{1}{2}[N_{M\alpha,N}\Delta q_\alpha + \\
&+ N_{N\alpha,M}\Delta q_\alpha + N_{K\alpha,M}\Delta q_\alpha N_{K\beta,N}q_\beta + N_{K\beta,M}\Delta q_\beta N_{K\alpha,N}\Delta q_\alpha] = \\
&= \Big[\frac{N_{M\alpha,N}+N_{N\alpha,M}}{2} + \frac{N_{K\alpha,M}N_{K\beta,N} + +N_{K\beta,M}N_{K\alpha,N}}{2}q_\beta\Big][\Delta q_\alpha] = \\
&= \Big([B^0_{MN\alpha}] + [B^{(NL}_{MN\alpha\beta})][q_\beta]\Big)[\Delta q_\alpha] = [B^*_{MN\alpha}][\Delta q_\alpha] = \mathbf{B}^*\Delta\boldsymbol{q} \\
\Delta\mathbf{S} &= [\Delta S_{KL}] = [C_{KLMN}][\Delta E_{MN}] = [C_{KLMN}][B^*_{MN\alpha}][\Delta q_\alpha] = \mathbf{CB}^*\Delta\boldsymbol{q} \\
\Delta\mathbf{T}_R &= \Delta\mathbf{S}(\mathbf{1}+\nabla\boldsymbol{u}) + \mathbf{S}\nabla(\Delta\boldsymbol{u}) = \qquad (3.3) \\
&= [\Delta S_{KL}][\delta_{iL} + N_{i\gamma,L}q_\gamma] + [S_{KL}][N_{i\alpha,L}][q_\alpha] = \\
&= [C_{KLMN}][B^*_{MN\alpha}][\Delta q_\alpha][\delta_{iL} + N_{i\gamma,L}q_\gamma] + [S_{KL}][N_{i\alpha,L}][\Delta q_\alpha] = \\
&= \Big([C_{KLMN}][B^*_{MN\alpha}][\delta_{iL} + N_{i\gamma,L}q_\gamma] + [S_{KL}][N_{i\alpha,L}]\Big)[\Delta q_\alpha] = \\
&= \Big\{[C_{KLMN}][B^0_{MN\alpha}][\delta_{iL}] + [C_{KLMN}]\Big([B^{(NL)}_{MN\alpha\beta}][q_\beta][\delta_{iL} + N_{i\gamma,L}q_\gamma]\Big) + \\
&+ [S_{KL}][N_{i\alpha,L}]\Big\}[\Delta q_\alpha] = [\Delta T_{Ki\alpha}][\Delta q_\alpha] = \\
&= (\mathbf{CB}^0\mathbf{1} + \mathbf{CB}^{**} + \mathbf{S}\Delta\mathbf{N})[\Delta q_\alpha]
\end{aligned}
$$

where the following matrices have been introduced

$$
\begin{aligned}
&\mathbf{B}^0 = [B^0_{MN\alpha}] = \Big[\frac{N_{M\alpha,N}+N_{N\alpha,M}}{2}\Big] \\
&\mathbf{B}^{(NL)} = [B^{(NL)}_{MN\alpha\beta}] = \Big[\frac{N_{K\alpha,M}N_{K\beta,N} + N_{K\beta,M} + N_{K\alpha,N}}{2}\Big] \\
&\mathbf{B}^*(\boldsymbol{q}) = [B^*_{MN\alpha}] = \Big([B^0_{MN\alpha}] + [B^{(NL)}_{MN\alpha\beta}][q_\beta]\Big) = \mathbf{B}^0 + \mathbf{B}^{(NL)}\boldsymbol{q} \\
&\mathbf{C} = [C_{KLMN}] \\
&\nabla\mathbf{N} = [N_{i\alpha,L}] = [\delta_{iK}N_{K\alpha,L}] = \\
&\qquad +[\delta_{iK}]\Big(\Big[\frac{N_{K\alpha,L}+N_{L\alpha,K}}{2}\Big] + \Big[\frac{N_{K\alpha,L}-N_{L\alpha,K}}{2}\Big]\Big) = \mathbf{1}(\mathbf{B}^0 + \mathbf{B}^A)
\end{aligned}
$$

$$\mathbf{B}^{**}(\boldsymbol{q}) = [B^{**}_{MN\alpha iL}] = [B^{(NL)}_{MN\alpha\beta}][q_\beta][\delta_{iL} + N_{i\gamma,L}q_\gamma] =$$
$$= \mathbf{B}^{(NL)}\boldsymbol{q}(1 + \nabla\mathbf{N}\boldsymbol{q}) = \mathbf{B}^{(NL)}\boldsymbol{q} + \mathbf{B}^{(NL)}\boldsymbol{q}\mathbf{B}^0\boldsymbol{q}$$

The finite element approximation of the virtual terms gives

$$\begin{aligned} &\delta\Delta\boldsymbol{u} = [N_{i\alpha}][\delta\Delta q_\alpha] && \delta\nabla(\Delta\boldsymbol{u}) = [N_{i\beta,K}][\delta\Delta q_\beta] \\ &\delta\Delta u_n = [N_{j\beta}n_j][\delta\Delta q_\beta] && \delta\Delta\boldsymbol{u}_T = [P_{ij}][N_{j\beta}][\delta\Delta q^+_\beta - \delta\Delta q^-_\beta] \end{aligned} \tag{3.4}$$

Substituting now all obtained expressions (3.1)-(3.4) into integrals (2.15), and taking into account the known result, that the multiplication of symmetric and skew matrices are equal to zero, we obtain

$$\begin{aligned} \Delta\delta U &= \int\limits_{V_R} \Delta\mathbf{T}_R : \delta\nabla(\Delta\boldsymbol{u})\, dV_R = \int\limits_{V_R} \Delta T_{Ki\alpha}\Delta q_\alpha N_{i\beta,K}\delta\Delta q_\beta\, dV_R = \\ &= \int\limits_{V_R} (\mathbf{CB}^0\mathbf{1} + \mathbf{CB}^{**} + \mathbf{S}\nabla\mathbf{N})\nabla\mathbf{N}\Delta\boldsymbol{q}\delta\Delta\boldsymbol{q}\, dV_R = \\ &= \int\limits_{V_R} (\mathbf{CB}^0\nabla\mathbf{N} + \mathbf{CB}^{**}\nabla\mathbf{N} + \mathbf{S}\nabla\mathbf{N}\nabla\mathbf{N})\, dV_R[\Delta q_\alpha][\delta\Delta q_\alpha] = \\ &= \int\limits_{V_R} (\mathbf{B}^{0T}\mathbf{CB}^0 + \mathbf{B}^{0T}\mathbf{CB}^{**} + \mathbf{S}\nabla\mathbf{N}\nabla\mathbf{N})\, dV_R\Delta\boldsymbol{q}\delta\Delta\boldsymbol{q} = \\ &= [\mathbf{K}_0 + \mathbf{K}_{(NL)}(\boldsymbol{q}) + \mathbf{K}_S(\boldsymbol{q})]\Delta\boldsymbol{q}\delta\Delta\boldsymbol{q} \\ \Delta\delta L &= \int\limits_{V_R} \rho_R\Delta\boldsymbol{b}\delta\Delta\boldsymbol{u}\, dV_R + \int\limits_{S_R} \Delta\boldsymbol{p}_R\delta\Delta\boldsymbol{u}\, dS_R = \\ &= \int\limits_{V_R} \rho_R\Delta b_i N_{i\alpha}\delta\Delta q_\alpha\, dV_R + \int\limits_{S_R} \Delta p_{Ri}N_{i\beta}\delta\Delta q_\beta\, dS_R = \\ &= \Big(\int\limits_{V_R} \rho_R\Delta b_i N_{i\beta}\, dV_R + \int\limits_{S_R} \Delta p_{Ri}N_{i\beta}\, dS_R\Big)\delta\Delta q_\beta = \\ &= [\Delta F^{ext}_\beta][\delta\Delta q_\beta] = \Delta\mathbf{F}^{ext}\delta\Delta\boldsymbol{q} \\ \Delta\delta L_B &= \int\limits_{V_R} \rho_R\Delta\ddot{\boldsymbol{u}}\delta\Delta\boldsymbol{u}\, dV_R = \int\limits_{V_R} \rho_R N_{i\alpha}\Delta\ddot{q}_\alpha N_{i\beta}\delta\Delta q_\beta\, dV_R = \end{aligned}$$

$$
\begin{aligned}
&= \Big[\int\limits_{V_R} \rho_R N_{i\alpha} N_{i\beta}\, dV_R\Big][\Delta\ddot{q}_\alpha][\delta\Delta q_\beta] = \\
&= [M_{\alpha\beta}][\Delta\ddot{q}_\alpha][\delta\Delta q_\beta] = \mathbf{M}\Delta\ddot{\boldsymbol{q}}\delta\Delta\boldsymbol{q}
\end{aligned}
$$

$$
\begin{aligned}
\Delta\delta L_n &= \int\limits_{\Gamma_c} \Delta t_n \delta\Delta u_n\, d\Gamma = -\frac{1}{\varepsilon}\int\limits_{\Gamma_c} N_{i\alpha} n_i \Delta q_\alpha N_{j\beta} n_j \delta\Delta q_\beta\, d\Gamma = \\
&= \Big[1\frac{1}{\varepsilon}\int\limits_{\Gamma_c} N_{i\alpha} N_{j\beta} n_i n_j\, d\Gamma\Big][\Delta q_\alpha][\delta\Delta q_\beta] = \\
&= [K^{CN}_{\alpha\beta}][\Delta q_\alpha][\delta\Delta q_\beta] = \mathbf{K}_{CN}\Delta\boldsymbol{q}\delta\Delta\boldsymbol{q}
\end{aligned}
$$

$$
\begin{aligned}
\Delta\delta L_T &= \int\limits_{\Gamma_c} \Delta\boldsymbol{t}_T \delta\Delta\boldsymbol{u}_T\, d\Gamma = \int\limits_{\Gamma_c}\Big\{-\Delta\mu t_n \phi_\varepsilon [P_{ij}][N_{j\alpha}][\dot{q}^+_\alpha - \dot{q}^-_\alpha] + \\
&+ \frac{\mu}{\varepsilon}\phi_\varepsilon [P_{ij}][N_{j\gamma}][\dot{q}^+_\gamma - \dot{q}^-_\gamma] N_{j\alpha} n_j \Delta q_\alpha - \\
&- \frac{\mu t_n}{\varepsilon}[P_{ij}][N_{j\alpha}][\Delta\dot{q}^+_\alpha - \Delta\dot{q}^-_\alpha]\Big\}[P_{iK}][N_{K\beta}][\delta\Delta q^+_\beta - \delta\Delta q^-_\beta]\, d\Gamma = \\
&= \Big\{\Big(-\phi_\varepsilon \int\limits_{\Gamma_c} P_{ij}\Delta\mu t_n N_{j\alpha} P_{iK} N_{K\beta}\, d\Gamma\Big)[\dot{q}^+_\alpha - \dot{q}^-_\alpha] + \\
&+ \Big(\frac{\mu}{\varepsilon}\phi_\varepsilon \int\limits_{\Gamma_c} P_{ij} N_{j\gamma} N_{K\alpha} n_K P_{il} N_{l\beta}\, d\Gamma\Big)[\dot{q}^+_\gamma - \dot{q}^-_\gamma][\Delta q_\alpha] + \\
&+ \Big(-\int\limits_{\Gamma_c} \frac{\mu t_n}{\varepsilon} P_{ij} N_{j\alpha} P_{iK} N_{K\beta}\, d\Gamma\Big)[\Delta\dot{q}^+_\alpha - \Delta\dot{q}^-_\alpha]\Big\}[\delta\Delta q^+_\beta - \delta\Delta q^-_\beta] = \\
&= \Big\{[K^\mu_{\alpha\beta}] + [K^{nT}_{\alpha\beta}][\Delta q_\alpha] + [K^T_{\alpha\beta}][\Delta\dot{q}^+_\alpha - \Delta\dot{q}^-_\alpha]\Big\}[\delta\Delta q^+_\beta - \delta\Delta q^-_\beta] = \\
&= \Big\{\mathbf{K}_\mu(\dot{\boldsymbol{q}}) + \mathbf{K}_{nT}(\dot{\boldsymbol{q}})\Delta\boldsymbol{q} + \mathbf{K}_T(\Delta\dot{\boldsymbol{q}}^+ - \Delta\dot{\boldsymbol{q}}^-)\Big\}[\delta\Delta\boldsymbol{q}^+ - \delta\Delta\boldsymbol{q}^-]
\end{aligned}
$$

$$
\begin{aligned}
\delta L_{\Delta\Gamma_c} &= \Big\{\int\limits_{\Gamma_c}\Big(\frac{\partial t_n}{\partial n} - 2kt_n\Big)\Delta\boldsymbol{\varphi}\cdot\boldsymbol{n}^-[N_{i\alpha} n_i]\, d\Gamma + \\
&+ \int\limits_{\partial\Gamma_c} t_n \boldsymbol{\nu}\cdot\Delta\boldsymbol{\varphi}[N_{i\alpha} n_i]\, ds\Big\}\delta\Delta q_\beta + \\
&+ \Big\{\int\limits_{\Gamma_c} \mathbf{P}\Big(\frac{\partial \boldsymbol{t}_T}{\partial n} - 2k\boldsymbol{t}_T\Big)\Delta\boldsymbol{\varphi}\cdot\boldsymbol{n}^- P_{ij} N_{j\beta}\, d\Gamma +
\end{aligned}
$$

$$+ \int_{\partial\Gamma_c} \mathbf{P}\boldsymbol{t}_T\boldsymbol{\nu} \cdot \Delta\boldsymbol{\varphi} P_{ij} N_{j\beta}\, ds \Big\} [\delta\Delta q_\beta^+ - \delta\Delta q_\beta^-] =$$

$$= [F_\beta^{\varphi_n}][\delta\Delta q_\beta] + [F_\beta^{\varphi_T}][\delta\Delta q_\beta^+ - \delta\Delta q_\beta^-] =$$

$$= \mathbf{F}_{\varphi_n} \cdot \delta\Delta\boldsymbol{q} + \mathbf{F}_{\varphi_T} \cdot (\delta\Delta\boldsymbol{q}^+ - \delta\Delta\boldsymbol{q}^-)$$

The following matrices have been introduced in the above

$\mathbf{K}_0$ – stiffness matrix

$$\mathbf{K}_0 = \int_{V_R} \mathbf{B}^{0T}\mathbf{C}\mathbf{B}^0\, dV_R$$

$\mathbf{K}_{NL}$ – stiffness supply matrix resulting from the strain nonlinearity

$$\mathbf{K}_{NL} = \int_{V_R} \mathbf{B}^{0T}\mathbf{C}\mathbf{B}^{**}\, dV_R$$

$\mathbf{K}_S$ – stiffness supply matrix resulting from the stresses

$$\mathbf{K}_S = \int_{V_R} \mathbf{S}\nabla\mathbf{N}\nabla\mathbf{N}\, dV_R$$

$\mathbf{M}$ – inertia matrix

$$\mathbf{M} = \int_{V_R} \rho_R \mathbf{N}^\top\mathbf{N}\, dV_R$$

$\mathbf{K}_{CN}$ – stiffness supply matrix resulting from the normal contact stresses

$$\mathbf{K}_{CN} = -\frac{1}{\varepsilon}\int_{\Gamma_c} N_{i\alpha}N_{j\beta}n_i n_j\, d\Gamma$$

$\mathbf{K}_\mu$ – friction matrix resulting from the friction coefficient

$$\mathbf{K}_\mu = -\phi_\varepsilon \int_{\Gamma_c} P_{ij}\Delta\mu t_n N_{j\alpha} P_{iK} N_{K\beta}\, d\Gamma(\dot{q}_\alpha^+ - \dot{q}_\alpha^-)$$

$\mathbf{K}_{nT}$ – stiffness supply matrix resulting from the friction

$$\mathbf{K}_{nT} = \frac{\mu}{\varepsilon}\int_{\Gamma_c} \phi_\varepsilon P_{ij} N_{j\gamma} N_{K\alpha} n_K P_{il} N_{l\beta} (\dot{q}_\gamma^+ - \dot{q}_\gamma^-)\, d\Gamma$$

K_T – damping matrix resulting from the friction

$$\mathsf{K}_T = -\frac{\mu t_n}{\varepsilon} \int\limits_{\Gamma_c} P_{ij} N_{j\alpha} P_{iK} N_{K\beta}\, d\Gamma$$

F_{φ_n} – contact domain residual matrix resulting from the normal contact stresses

$$\mathsf{F}_{\varphi_n} = \int\limits_{\Gamma_c} \Big(\frac{\partial t_n}{\partial n} - 2kt_n\Big) N_{i\beta} n_i \Delta\varphi_K n_K\, d\Gamma + \int\limits_{\partial\Gamma_c} t_n N_{i\beta} n_i \nu_j \Delta\varphi_J\, dS$$

F_{φ_T} – contact domain residual matrix resulting from the friction

$$\mathsf{F}_{\varphi_T} = \int\limits_{\Gamma_c} P_{iK} \Big(\frac{\partial t_{TK}}{\partial n} - 2kt_{TK}\Big) P_{ij} N_{j\beta} \Delta\varphi_l n_l\, d\Gamma + \int\limits_{\partial\Gamma_c} P_{iK} t_{TK} P_{ij} N_{j\beta} \varphi_l \Delta\varphi_l\, dS$$

$\Delta\mathsf{F}^{ext}$ – external force matrix

$$\Delta\mathsf{F}^{ext} = \int\limits_{V_R} \rho_R \mathbf{N} \Delta\boldsymbol{b}\, dV_R + \int\limits_{S_R} \mathbf{N} \Delta\boldsymbol{p}_R\, dS_R$$

Substituting all the obtained expressions into virtual power equation (2.15) and taking into account the fact that it must be fulfilled for all virtual increments $\delta\Delta q_\beta$, $\beta = 1, ..., N$, where N is the global number (after aggregation) of the unknowns, we finally obtain the matrix equation

$$\begin{aligned} &\mathsf{M}\Delta\ddot{\boldsymbol{q}} + \mathsf{K}_T(\boldsymbol{q})\Delta\dot{\boldsymbol{q}} + [\mathsf{K}_0 + \mathsf{K}_{NL}(\boldsymbol{q}) + \mathsf{K}_S(\boldsymbol{q}) + \mathsf{K}_{nT}(\dot{\boldsymbol{q}}) + \mathsf{K}_{CN}]\Delta\boldsymbol{q} = \\ &= \Delta\mathsf{F}^{ext} + \mathsf{K}_\mu(\dot{\boldsymbol{q}}) + \mathsf{F}_{\varphi_n}(\boldsymbol{q}) + \mathsf{F}_{\varphi_T}(\dot{\boldsymbol{q}}) \end{aligned} \tag{3.5}$$

The matrix K_{nT} is non-symmetric since it results from the terms containing product of the displacements normal and tangent to the boundary velocities. The matrices $\mathsf{K}_{NL}(q)$ and $\mathsf{K}_S(q)$ follow from the presence of large deformations. The matrix K_{CN} is responsible for the normal contact whereas K_T and K_μ represent the influence of friction. The vectors F_{φ_n} and F_{φ_T} represent these parts of reaction of the system, which are induced by the changes of the contact zone during the deformation. So, equation (3.5) contains all terms which characterize the properties of the dynamic frictional contact of bodies undergoing large deformations. The solution to system (3.5) must be accompanied by a procedure of determination of the current contact zone Γ_c^t. This can be done by the following iterative approach: in each time step one considers two separate problems:

stage I – assumes that the tangent stresses $\boldsymbol{t}_T$ are known (from the previous iteration). This makes it possible to solve (3.5) in a much more simple form

$$\mathbf{M}\Delta\ddot{\boldsymbol{q}}+\mathbf{K}_T\Delta\dot{\boldsymbol{q}}+(\mathbf{K}_0+\mathbf{K}_{NL}+\mathbf{K}_S+\mathbf{K}_{CN})\Delta\boldsymbol{q}=\Delta\mathbf{F}^{ext}+\mathbf{F}_{\varphi_n}+\Delta\mathbf{R}_I \quad (3.6)$$

where $\Delta\mathbf{R}_I$ denotes the sum of all known terms depending on friction. Solving (3.6), we obtain $\Delta\boldsymbol{q}$ and hence Δt_n, t_n and Γ_c.

stage II – having Γ_c and t_n obtained we look for the new $\boldsymbol{t}_T$ by considering the equation

$$\mathbf{M}\Delta\ddot{\boldsymbol{q}}+\mathbf{K}_T\Delta\dot{\boldsymbol{q}}+(\mathbf{K}_0+\mathbf{K}_{NL}+\mathbf{K}_S)\Delta\boldsymbol{q}=\Delta\mathbf{F}^{ext}+\Delta\mathbf{R}_{II} \quad (3.7)$$

The term $\Delta\mathbf{R}_{II}$ means now the sum of all terms known from the previous stage.

Both procedures of solving are being repeatedly carried out until the differnces between $\Delta\boldsymbol{q}^I$ and $\Delta\boldsymbol{q}^{II}$ (and hence the corresponding zones Γ_c^i, Γ_c^{II}) for both stages are small enough (with the demanded accuracy). In such a way we omit the difficulties connected with the asymmetry of the matrix $\mathbf{K}_{nT}$. This fact enables us to use the standard procedure of solving the linear system of equations (with symmetrical matrices). Then we pass to the next time step $t+\Delta t$. To solve (3.5) numerically, different time integration methods can be used. We decided to apply the implicit Newmark method with the obviously used parameters $\alpha = 0.25$ and $\beta = 0.5$. Thus, it is convenient to write equation (3.5) in the form

$$\mathbf{M}\ddot{\boldsymbol{q}}^{t+\Delta t}+\mathbf{K}_T^t\Delta\dot{\boldsymbol{q}}+\mathbf{K}^*\Delta\boldsymbol{q}=\mathbf{F}_{ext}^{t+\Delta t}+\mathbf{R}^*+\mathbf{M}\ddot{\boldsymbol{q}}^t-\mathbf{F}_{ext}^t \quad (3.8)$$

where $\mathbf{K}^*$ is the global stiffness matrix

$$\mathbf{K}^*=\mathbf{K}+\mathbf{K}_{NL}+\mathbf{K}_S+\mathbf{K}_{nT}+\mathbf{K}_{CN}$$

and $\mathbf{R}^*$ – residual column-matrix resulting from the increment of contact terms

$$\mathbf{R}^*=\mathbf{K}_\mu\dot{\boldsymbol{q}}+\mathbf{F}_{\phi_n}+\mathbf{F}_{\phi_T}$$

Knowing that for the instant t (i.e. for the configuration B_N) equation (2.1) must be fulfilled, one can write

$$\mathbf{Q}^t=\mathbf{F}_{ext}^t-\mathbf{M}\ddot{\boldsymbol{q}}^t+\mathbf{F}_T^t+\mathbf{F}_n^t \quad (3.9)$$

where the members

$$\mathbf{Q}^t = [Q_\beta] = \int_{V_R} T_{Ki} N_{i\beta,K}\, dV_R \qquad \mathbf{F}_T^t = [F_\beta^T] = \int_{\Gamma_c} t_{Ti} P_{ij} N_{j\beta}\, d\Gamma$$

$$\mathbf{F}_n^t = [F_\beta^n] = \int_{\Gamma_c} t_n N_{i\beta} n_i\, d\Gamma$$

result directly from (2.1) after substituting (3.4).

Hence, governing equation (3.8) finally takes the form

$$\mathbf{M}\ddot{\boldsymbol{q}}^{t+\Delta t} + \mathbf{K}_T^t \Delta\dot{\boldsymbol{q}} + \mathbf{K}_*^t \Delta\boldsymbol{q} = \mathbf{F}_{ext}^{t+\Delta t} + \mathbf{R}_*^t + \mathbf{F}_T^t + \mathbf{F}_n^t - \mathbf{Q}^t \tag{3.10}$$

suitable for direct application of the Newmark formula.

4. Numerical examples

4.1. Rubber block undergoing kinematic excitation

Consider a rubber block $a \times b = 0.48 \times 0.5\,\mathrm{m}$ resting on a rigid foundation (Fig. 2). For simplicity, the material of the rubber is treated as an elastic one with Young's modulus $E = 5\,000\,\mathrm{KN/m^2}$, Poisson's ratio $\nu = 0.45$ and density $\rho = 1.7 \cdot 10^3\,\mathrm{kg\,m^3}$. The block being in equilibrium at the initial instant t_0, is assumed to be excited by the prescribed vertical and horizontal displacements $u_{0y} = 0.05\,\mathrm{m}$, $u_{0x} = v_{0x}t$, $v_{0x} = 1\,\mathrm{m/s}$ on the upper edge (see Fig. 2). The side-edges are free of loads. Three friction models have been taken into account:

- Coulomb-Amonton's law with the constant but sufficient large friction coefficient $\mu = 1.0$
- Coulomb's model with the variable friction coefficient according to the Grosch-Schallamach formula $\mu = \mu_0 (t_n/E)^{1/9}$, $\mu_0 = 1$
- compliance model with the parameters

$$\begin{array}{llll} m_N = 1 & m_T = \dfrac{8}{9} & c_N = 10^4 & \\ m_N = 2 & m_T = \dfrac{16}{9} & c_N = 10^8 & c_T = c_N^{8/9} E^{1/9} \\ m_N = 3 & m_T = \dfrac{8}{3} & c_N = 10^{12} & \end{array}$$

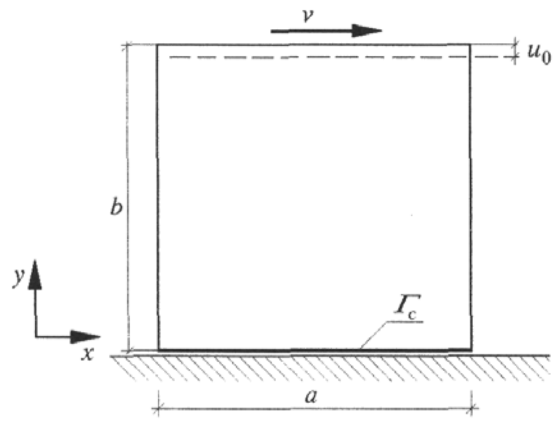

Fig. 2.

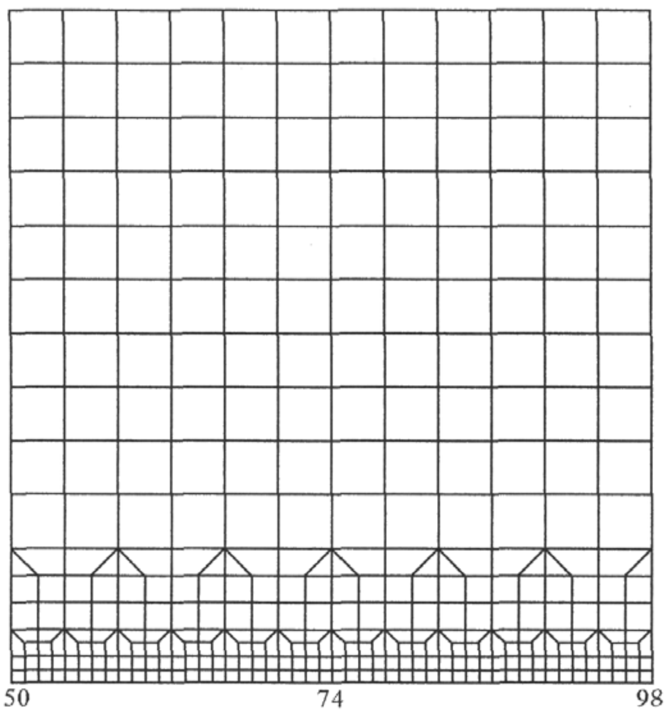

Fig. 3. Discretization by FE

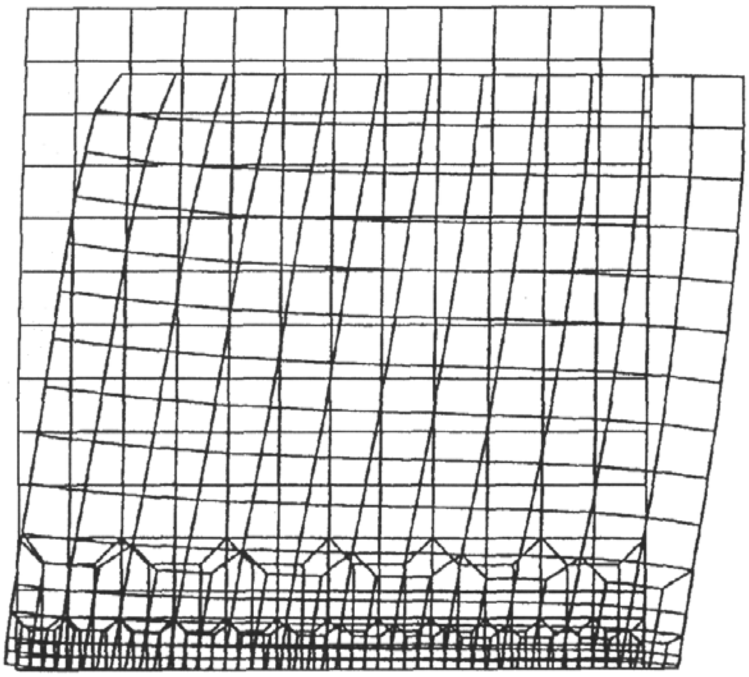

Fig. 4. Deformation at $t = 0.07\,\mathrm{s}$

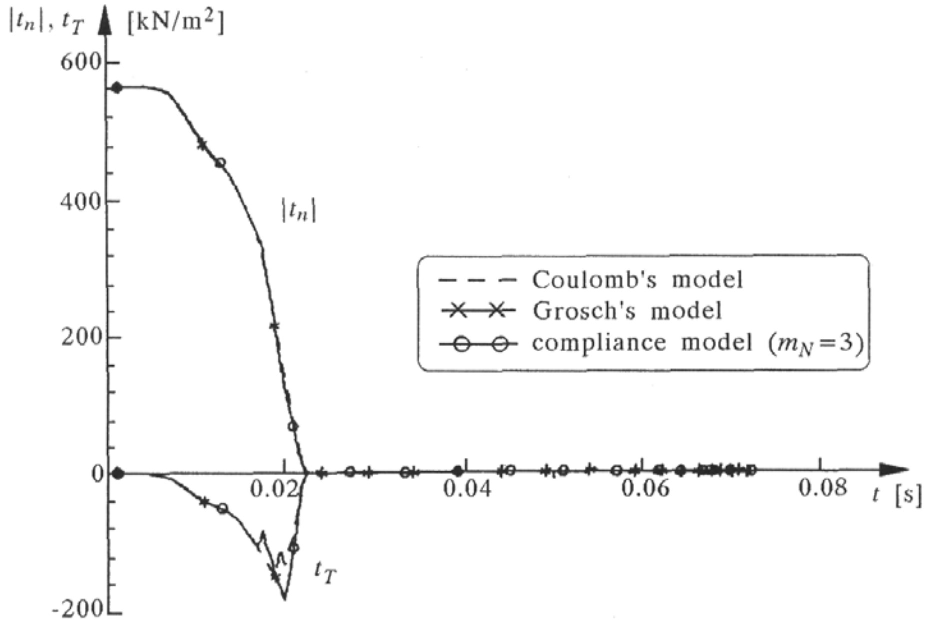

Fig. 5. Contact stresses at node 50 for different friction models

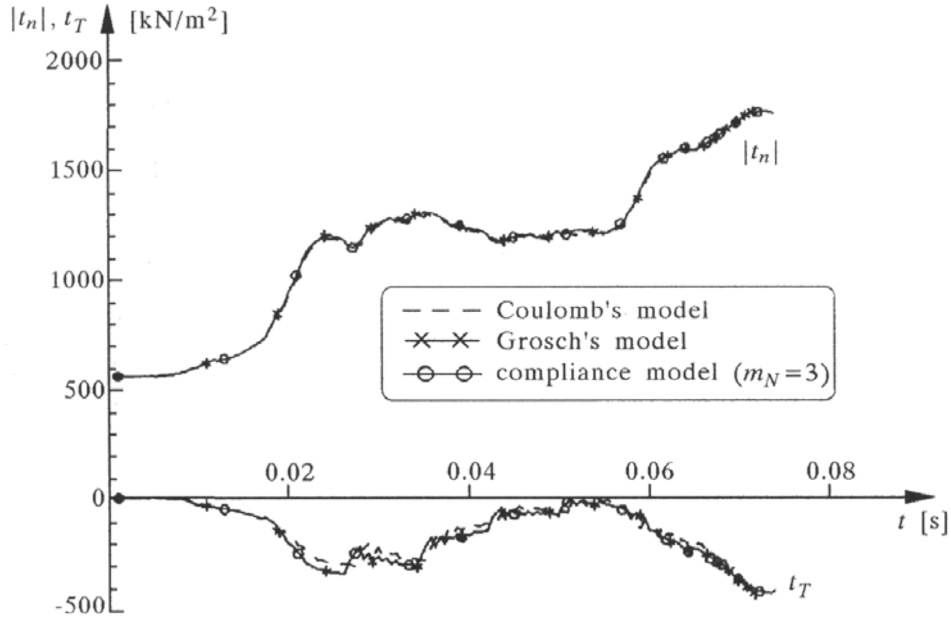

Fig. 6. Contact stresses at node 98 for different friction models

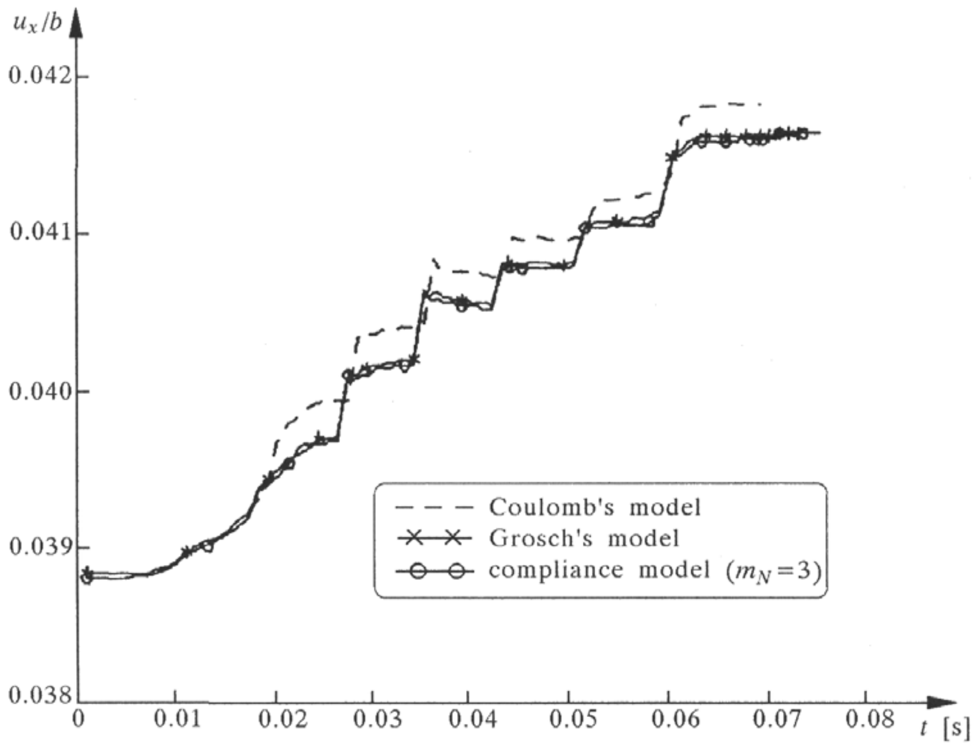

Fig. 7. Horizontal displacement of node 98 for different friction models

Numerical results are shown on Fig. 4-7, which demonstrate the behaviour of the system during the time interval [0-0.07] s. The plots of contact stresses at node 50 show stiction at the beginning and then separation for all considered models of friction. This character of stress distribution coincide with the deformation of the block (Fig. 4). It is to be emphasized, that the zero values of the friction at the initial instant $t_0 = 0$ (see Fig. 5 and Fig. 6) results from the initial condition.

Point 98 being in permanent contact with the foundation (see Fig. 4 and Fig. 6) demonstrates a stick-slip process (Fig. 7).

4.2. Vibration of a concrete block resting on an elastic stratum

A block with dimensions $a \times b = 1.0 \times 0.5\,\mathrm{m}$ is loaded by forces as it is shown in Fig. 8.

The following data have been used:

— for concrete

$$E_b = 2.3 \cdot 10^{11}\,\frac{\mathrm{N}}{\mathrm{m}^2} \qquad \nu = 0.16 \qquad \rho = 2.2 \cdot 10^3\,\frac{\mathrm{kg}}{\mathrm{m}^3}$$

— for the foundation (soil)

$$E_g = 2.3 \cdot 10^{11}\,\frac{\mathrm{N}}{\mathrm{m}^2} \qquad \nu = 0.3 \qquad \rho = 1.8 \cdot 10^3\,\frac{\mathrm{kg}}{\mathrm{m}^3}$$

and

$$P_y = 300\,\mathrm{KN} \qquad P_x = 80\,KN$$

The initial conditions: the static frictionless indentation under P_y and own weight, $\dot{\boldsymbol{u}}(\boldsymbol{X}, 0) = \mathbf{0}$.

Friction for the Coulomb model with $\mu = 1.2$.

Fig. 11 shows an evident swaying process of the block evoked by the short-time load P_x. The middle point C demonstrates a stable vertical displacement with a value which results from the initial state. The vibrational character of motion of the system is visible also from the contact stress diagrams in Fig. 12 and from the phase plane plot in Fig. 13.

5. Conclusions

The numerical statement and analysis of the dynamic large deformation contact problem with friction have been considered. To omit the difficulties

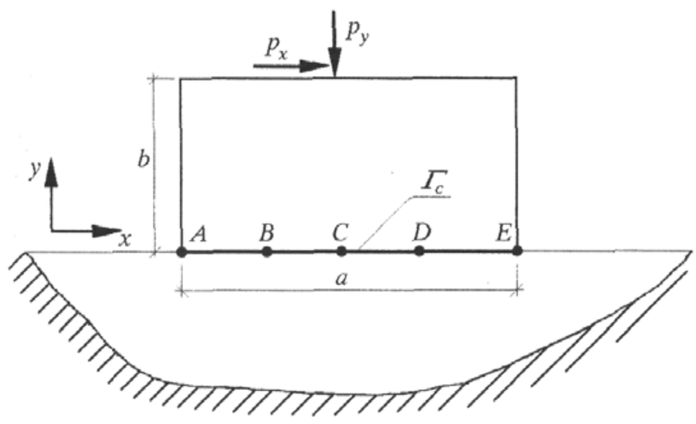

Fig. 8.

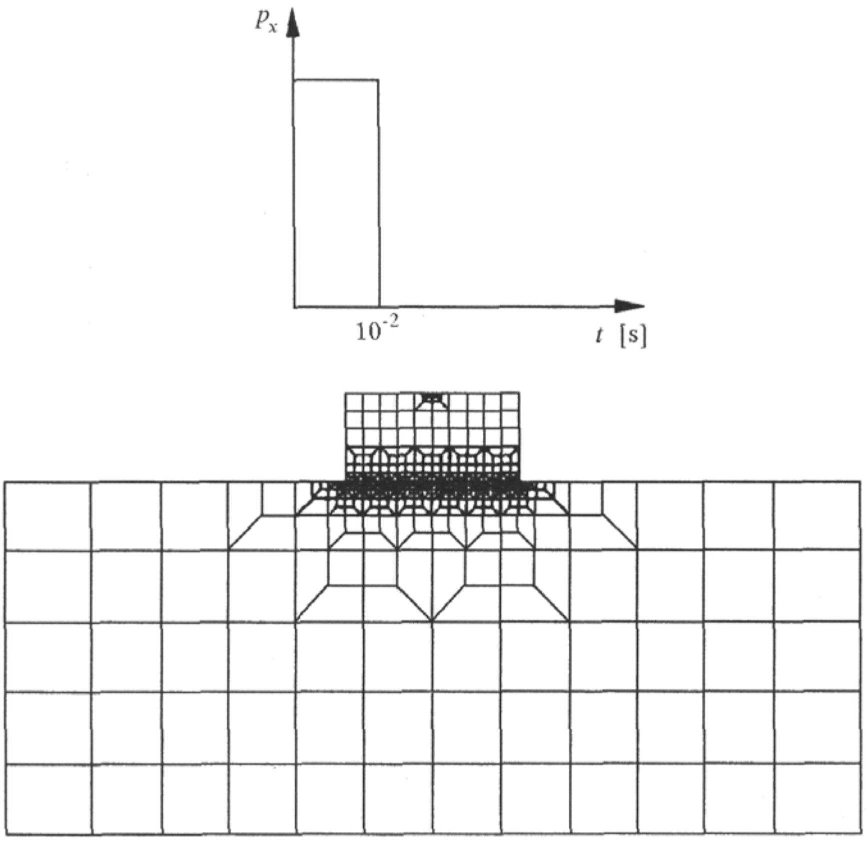

Fig. 9. FE mash and time dependence of the horizontal load

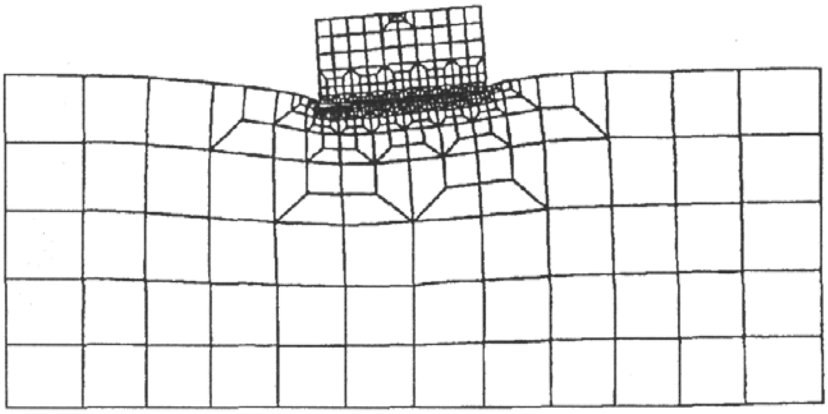

Fig. 10. Indentation of the block at time $t = 0.094\,\mathrm{s}$

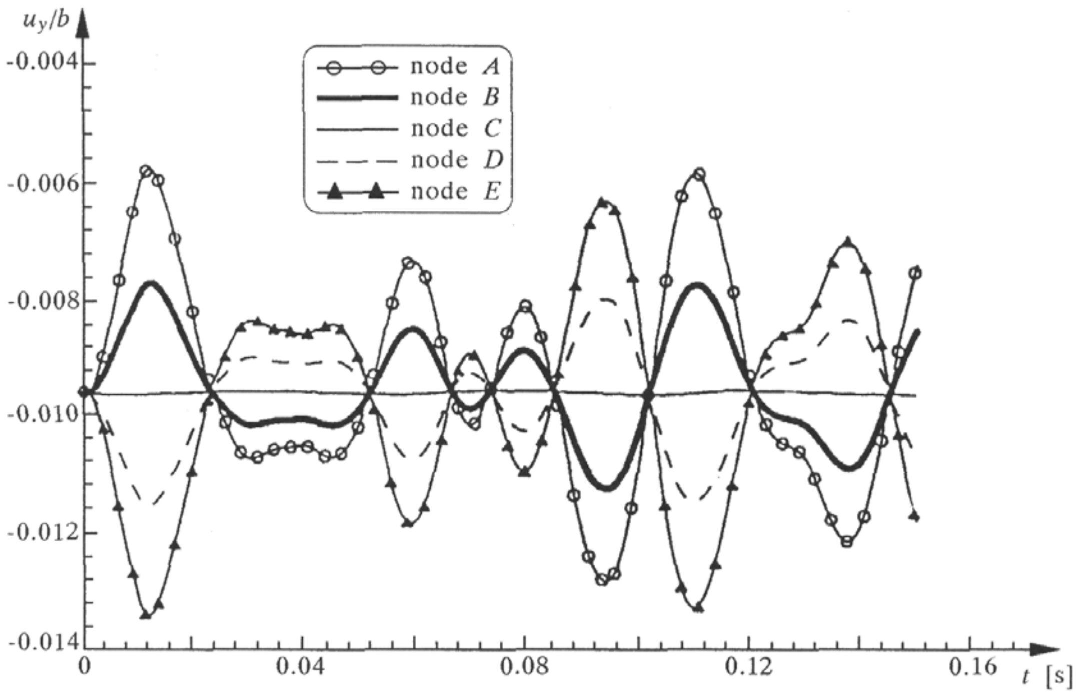

Fig. 11. Vertical vibrations of nodes of the contact zone

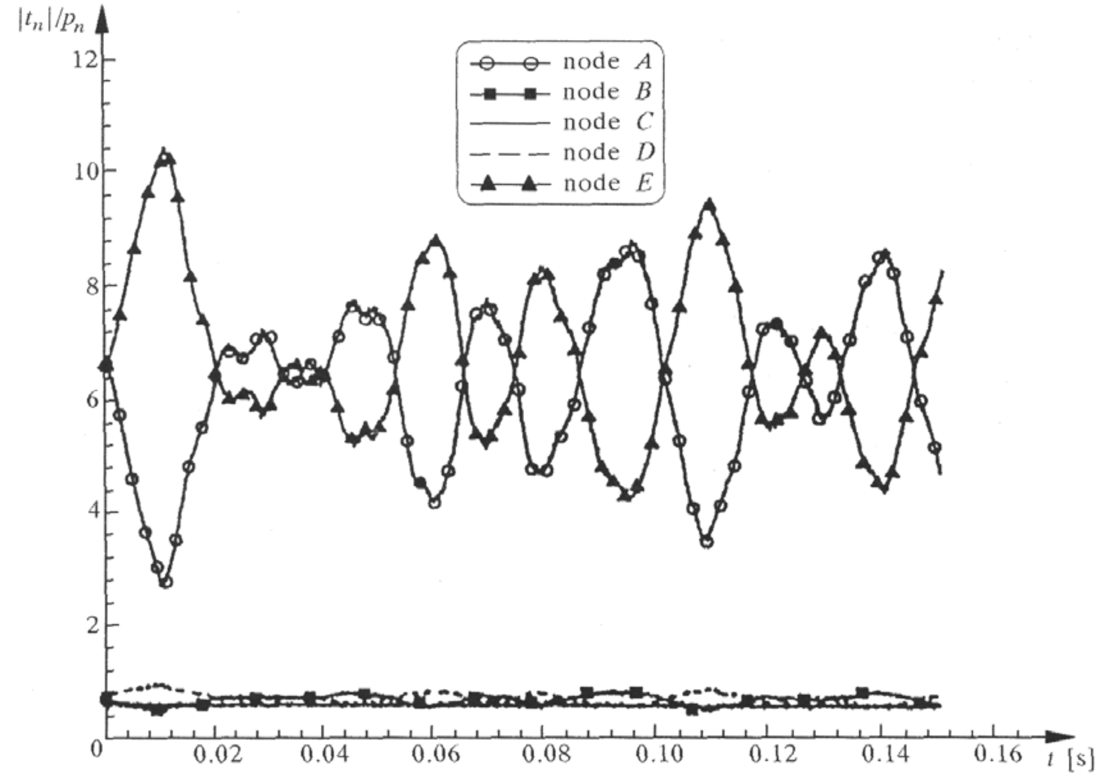

Fig. 12. Normal contact stresses of nodes

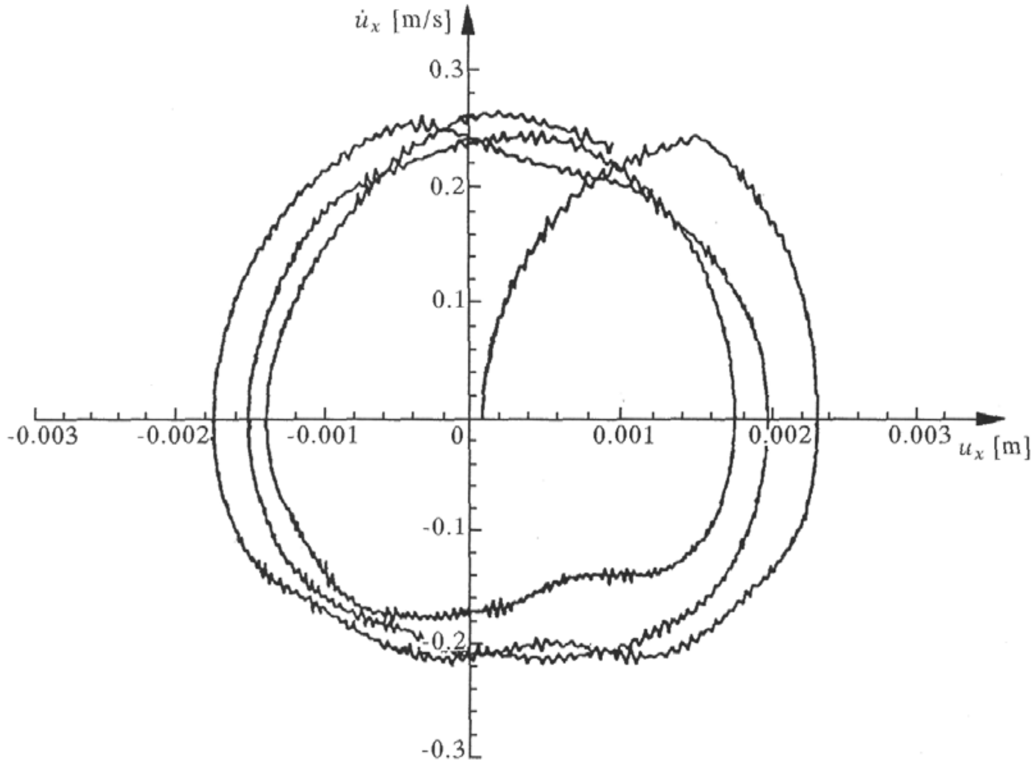

Fig. 13. Phase plane plot for the horizontal displacement of node A

connected with the asymmetric matrix $\mathbf{K}_{nT}$ resulting from friction a two-stage iterative procedure has been proposed. This approach has proved to be effective in determining the unknown zone. The numerical examples show that larger values of the friction coefficient ($\mu \sim 1$) require more time-consuming calculations. The compliance model of the contact response has proved to be more convenient in the calculations in comparision with the Signorini unilateral conditions and with the Coulomb law. It is also worth mentioning that the allowance for large deformations is suitable not only in the case of high elastic materials (example 4.1) but also for small deformations (example 4.2), where the nonlinear description leads to more accurate results (the displacements are smaller than those which results from the linear description).

References

1. CURNIER A., HE Q., TELEGA J., 1994, Continuum mechanics modelling of large deformation contact with friction, *Contact Mechanics Intern. Symp. (CMIS-II)*, Carry-le Rovet
2. HE Q., TELEGA J., CURNIER A., 1996, Unilateral contact of two solids subject to large deformations: formulation and existence results, *Proc. R. Soc. London*, A, **452**, 2691-2717
3. JARUSEK J., 1999, Dynamic contact problems with small Coulomb friction for viscoelastic bodies. Existence of solution, *Math. Models and Math. Appl. Sciences*, **9**, 1, 11-34, World Scient. Publ.
4. KLARBING A., 1995, Large displacement frictional contact: a continum framework for finite element discretization, *Eur. J. Mech. a/Solides*, **14**, 237-253
5. KLARBING A., BJÖRKMAN G., 1992, Solution of large displacement contact problems with friction using Newton's method for generalized equations, *Int. J. Num. Math. Engin.*, **34**, 249-269
6. LAURSEN T., 1994, The convected description in large deformation frictional contact problems, *Int. J. Solid Structures*, **31**, 5, 669-681
7. LAURSEN T, SIMO J., 1993a, A continum based finite element formulation for the implicit solution of multibody, large deformation frictional contact problems, *Int. J. Num. Meth. Engin.*, **36**, 3451-3485
8. LAURSEN J., SIMO J., 1993b, Algorithmic symmetrization of Coulomb friction problems using augmented Lagrangians, *Comp. Math. Appl. Mech. Eng.*, **108**, 133-146
9. LEBON F., RAOUS M., 1992, Multibody Contact Problem Including Friction in Structure Assembly, *Comp. and Struct.*, **43**, 5, 925-934

10. ODEN J., MARTINS J., 1985 Models and computational methods for dynamic friction phenomena, *Comp. Meth. Appl. Mech. Eng.*, **52**

11. RAOUS M., EDIT., 1988, Numerical Methods in Mechanics of Contact Involving Friction, *Special Issue to J. Mecanique Theorique et Appliquee*, Suppl. **7**, 1

12. SZEFER G., JASIŃSKA D., SALAMON J., 1994, Concept of a singular surface in contact mechanics, *Arch. Mech.*, **46**, 4,581-603

13. SZEFER G., 1997, Dynamic contact of bodies experiencing large deformation, *Acta Mechanica*, **125**, 217-233

14. SZEFER G., 1998, Contact problems in terms of large deformations, *ZAMM*, **78**, 8, 523-533

15. WRIGGERS P., VU VAN T., STEIN E., 1990, Finite element formulation of large deformation impact-contact problems with friction, *Comp. and Struct.*, **37**

16. ZHONG Z., 1993, *Finite element procedures for contact-impact problems*, Oxford Univ. Press

Dynamiczna analiza kontaktu ciał sprężystch przy dużych deformacjach

Streszczenie

W pracy przedstawiono analizę numeryczną dynamicznych zagadnień kontaktowych w obecności tarcia dla dużych deformacji. Ponieważ problemy tego typu odznaczają się silną nieliniowością rozważono szczegółowo przyrostowy opis wszystkich członów kontaktowych. Rozpatrzono różne modele tarcia.

Manuscript received May 21, 2001; accepted for print October 19, 2001